

Spectral reconstruction of Euclidean correlator moments in lattice QCD

JOHN BULAVA

FOR THE BARYON SCATTERING (BASC) COLLABORATION

Fakultät für Physik und Astronomie, Institut für Theoretische Physik II, Ruhr-Universität Bochum, 44780 Bochum, Germany

Summary. — A novel application of lattice QCD spectral reconstruction is presented, in which euclidean correlation function data in a fixed time range are used to infer values outside the range, enabling a model-independent investigation of the asymptotic large-time behavior. Moments of the correlator are also determined, and reconstructed correlation matrices between different moments are included in a variational optimization similar to the standard Generalized Eigenvalue Problem (GEVP). These ideas are illustrated using a single-nucleon correlation function determined on an $N = 2 + 1$ ensemble of gauge configurations at $m_\pi = 200\text{MeV}$.

In a finite spatial volume, the spectrum of QCD is discrete. The energy gaps suggest a strategy for the study of low-lying states in lattice QCD: take the large-time limit of Euclidean correlation functions to suppress unwanted excited state contamination. Solutions of a Generalized Eigenvalue Problem [1] can be used to construct correlators asymptotically dominated by a single state. However, (nearly) all correlation functions suffer from an exponential degradation of the signal-to-noise ratio with increasing Euclidean time [2, 3]. Unfortunately, in practice the most precise data at early times is discarded to fit the large-time region to a few-state ansatz. Choosing the lower bound for such fits is often delicate: the statistical error can be decreased at the expense of increased systematic error due to excited state contamination. It is possible that this interplay is (at least partly) responsible for the long-standing difficulty in reproducing the experimental value for the nucleon axial charge [4, 5].

A model-independent alternative to discarding the early-time data is presented here. It is based on the spectral reconstruction approach proposed by Backus and Gilbert [6] and first used in lattice QCD by Hansen, Lupo, and Tantalo [7]. Ref. [8] is similar in spirit to this work and is demonstrably of comparable effectiveness [9]. Other approaches to spectral reconstruction in lattice QCD are reviewed in Ref. [10]. The general problem

of spectral reconstruction employs Euclidean two-point correlator data

$$(1) \quad C(t) = \int d\omega \rho(\omega) e^{-\omega t}, \quad \rho(\omega) = \sum_n A_n \delta(\omega - E_n)$$

known for integer values of t/a in the range $t \in [t_{\min}, t_{\max}]$ with statistical errors. The direct determination of $\rho(\omega)$ from the correlator data is an ill-posed problem, which can be ameliorated by instead seeking smeared spectral densities of the form $\tilde{\rho}[f] = \int d\omega f(\omega) \rho(\omega)$ with a particular smearing kernel $f(\omega)$ specified *a priori*. Previous applications of Ref. [7] use $f(\omega)$ to approximate the Dirac- δ distribution [11], Heaviside step function [12], or implement the principle-value prescription [13]. This work however determines correlator moments, defined as

$$(2) \quad D(\alpha, \tau) = \int d\omega \rho(\omega) \omega^\alpha e^{-\omega \tau}.$$

The different symbol emphasizes that τ need not be constrained to the values of t provided by the data, suggesting that the temporal resolution may be increased with non-integer τ/a and the asymptotic limit probed with $\tau > t_{\max}$. Furthermore, taking the (rational) power α different from zero suppresses or enhances excited state contamination. Correlators with different α may be viewed as employing different interpolating operators, which can accordingly form a correlation matrix for use in a Generalized eigenvalue problem (GEVP).

The reconstruction approach employed here is detailed in Ref. [7], with further discussion of the reliable estimation of statistical and systematic errors in Refs. [11, 14]. Consider an estimator for $D(\alpha, \tau)$ from Eq. 2 which is a linear combination of all input correlator timeslices

$$(3) \quad \hat{D}(\alpha, \tau) = \sum_{t=t_{\min}}^{t_{\max}} g_t(\alpha, \tau) C(t) \equiv \int d\omega \hat{f}(\omega) \rho(\omega).$$

Evidently $\hat{D}(\alpha, \tau)$ is a smeared spectral density smeared with the kernel $\hat{f}(\omega) = \sum_t g_t(\alpha, \tau) e^{-\omega t}$, in contrast to $D(\alpha, \tau)$ which is smeared with $f(\omega) = \omega^\alpha e^{-\omega \tau}$. Any difference between $\hat{f}(\omega)$ and $f(\omega)$ is a systematic error in the estimator $\hat{D}(\alpha, \tau)$. The systematic and statistical errors are quantified by

$$(4) \quad A[g] = \int_{\omega_0}^{\infty} d\omega \left\{ f(\omega) - \hat{f}(\omega) \right\}^2, \quad B[g] = \sum_{tt'} g_t g_{t'} \text{Cov} \{ C(t), C(t') \},$$

respectively. The coefficients $\{g_t\}$ are chosen to balance these two considerations by minimizing $G_\lambda[g] = (1 - \lambda)A[g] + \lambda B[g]$ for a particular $\lambda \in [0, 1]$. Small λ results in a reconstructed kernel $\hat{f}(\omega)$ close to the desired one $f(\omega)$, but at the expense of large statistical error. Large λ gives a statistically precise result, but with a large systematic error due to the difference between $\hat{f}(\omega)$ and $f(\omega)$. As is customary in lattice QCD data analysis, an ideal λ is sought in the statistics-limited regime wherein the systematic error is reliably smaller than the statistical error.

To test these ideas, a single-nucleon correlator from an $N_f = 2 + 1$ ensemble of gauge configurations with $m_\pi = 200$ MeV is employed. This correlator is computed over the

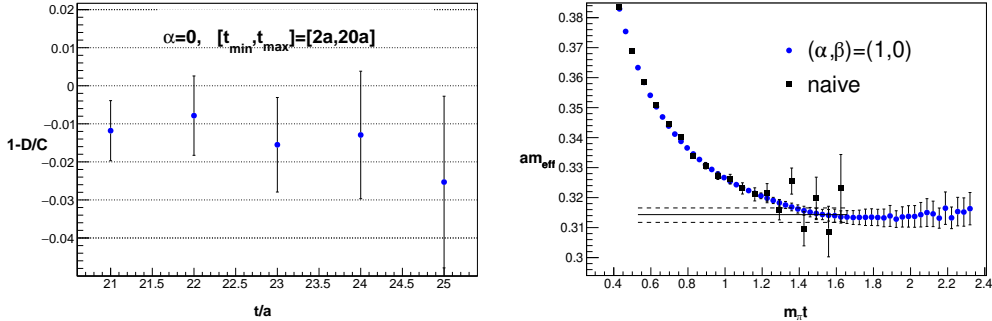


Fig. 1.: Two tests of the correlator reconstruction procedure. **Left**: using correlator data from times $t/a = [2, 20]$ to infer $D(0, t)$ at later times and compare with direct measurements of $C(t)$. The error on the relative difference between these two estimators is computed using the bootstrap procedure. **Right**: using times $t/a = [2, 25]$ to infer the effective mass using Eq. 5 with $(\alpha, \beta) = (1, 0)$. The naive forward-difference definition is also shown for comparison. The horizontal band is the result of a two-state fit (from Ref. [15]) over the horizontal range shown.

time range $[t_{\min}, t_{\max}] = [2a, 25a]$ and was used to determine the nucleon mass m_N in Ref. [15]. Further details of the interpolating operators and measurement procedure can be found there. For the reconstruction, the lower bound of the integration in Eq. 4 is fixed at $a\omega_0 = 0.3$, and the optimal λ chosen as in Ref. [14] by demanding that the variation of the estimator among a set of reconstructions which impose different constraints is three times smaller than the statistical error. As a first test of the procedure, a reconstruction is performed using timeslices $[t_{\min}, t_{\max}] = [2a, 20a]$ to infer $t = 21a, \dots, 25a$. The results of this test are shown in the left panel of Fig. 1, which demonstrates that the standard estimator for the correlator and $D(0, \tau)$ agree within 1.5σ .

Consider now the family of effective masses

$$(5) \quad m_{\text{eff}}(\alpha, \beta|\tau) = \left\{ \frac{D(\alpha, \tau)}{D(\beta, \tau)} \right\}^{1/(\alpha-\beta)}$$

for which $\lim_{\tau \rightarrow \infty} m_{\text{eff}}(\alpha, \beta|\tau) = m_N \times \{1 + O(e^{-2m_\pi \tau})\}$. Due to the finite spatial volume, the lowest non-interacting p -wave state has an energy close to $m_N + 2m_\pi$. The case $(\alpha, \beta) = (1, 0)$ coincides with the standard forward-difference effective mass up to $O(a^2)$ while different (α, β) have varying excited state contamination. A second test of the reconstruction procedure is shown in the right panel of Fig. 1, which compares the forward difference effective mass with $(\alpha, \beta) = (1, 0)$. The reconstructed effective mass is considerably more precise at later times, and asymptotically agrees with the value obtained from a two-state fit. It should be emphasised, however, that the spectral reconstruction approach does not impose a model for the time dependence.

Fig. 2 shows various (α, β) . A significant enhancement or reduction of the excited state contamination is evident similar to a variation in the level of quark field smearing, but here achieved for a single correlator. This naturally suggests employing different moments in a correlation matrix $A_{ij}(t) = D(\alpha_i + \alpha_j, t)$. Rather than the standard GEVP, which employs a second metric timeslice t_0 , the variation optimization is applied

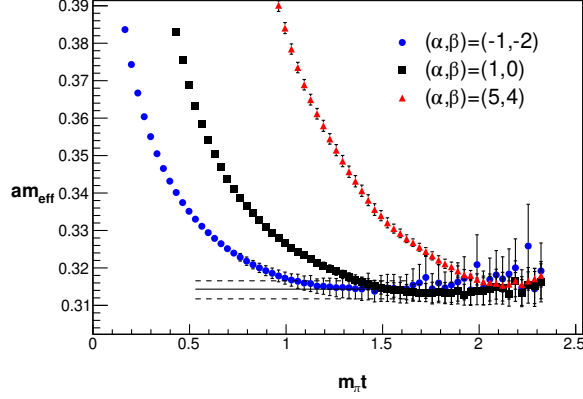


Fig. 2.: Different definitions of the effective mass by varying α and β in Eq. 5. In this manner the excited state contamination can be suppressed or enhanced relative to the conventional definition, which employs $(\alpha, \beta) = (1, 0)$.

directly to $B_{ij}(t) = D(\alpha_i + \alpha_j + 1, t)$, using $A(t)$ as a metric. This ‘equal-time’ GEVP is therefore

$$(6) \quad B(t)v_n(t) = \lambda_n(t)A(t)v_n(t),$$

where the eigenvalues $\lambda_n(t)$ approach directly the states of interest for large t . The results from a two-dimensional equal-time GEVP are shown in Fig. 3, which show a further reduction in excited state contamination compared to the input ‘diagonal’ effective masses. Furthermore, a rough estimate of the first excited state is provided with an energy near $m_N + 2m_\pi$. Interactions likely shift the multi-hadron excited states significantly from these naive expectations, however.

In conclusion, the reconstruction of correlator moments presented here provides model-independent determinations of the correlator at arbitrary Euclidean time separations.

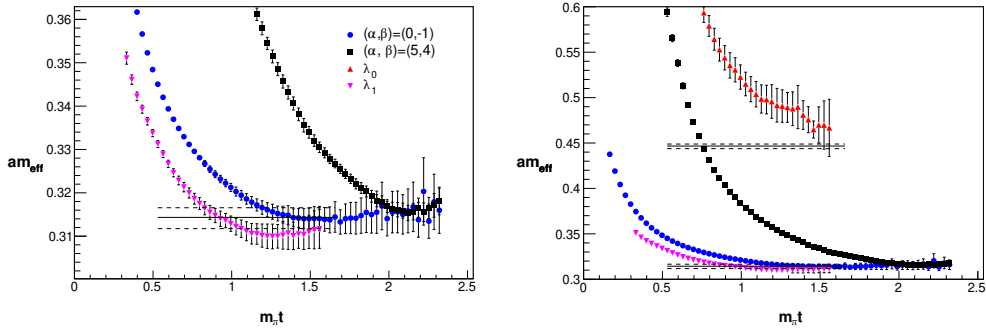


Fig. 3.: The eigenvalue $\lambda_n(t)$ from a two-by-two GEVP as in Eq. 6 with $\{\alpha_1, \alpha_2\} = \{-0.5, 2\}$. The lower horizontal band is the two-state fit from Ref. [15], as in Fig. 1. The right panel is zoomed out to show $\lambda_1(t)$, and the upper horizontal band is $m_N + 2m_\pi$.

Unlike few-state fits, these estimates employ the entire range of correlator data, including those at precise early times. However, no miracle has been achieved: the asymptotic behaviour shown in Figs. 1, 2, and 3 is consistent with a two-state fit and has a similar statistical precision. Nonetheless, it serves as a valuable model-independent confirmation of the two-state ansatz over the limited time range of input correlator data. In addition to the investigation of large-time asymptotics detailed here, the model-independent interpolation of correlator data may be useful in the comparison of lattice QCD vector-vector correlators and smeared experimental R -ratio data. It is likely that this approach can also be extended to treat the simultaneous reconstruction of multiple correlation functions in analogy to the ratios constructed to determine energy differences, as well as three-point correlation functions.

* * *

I thank my co-authors of Ref. [15] and my colleagues in the Baryon Scattering Collaboration (BaSc) for sharing the single-nucleon correlator used here.

REFERENCES

- [1] C. Michael and I. Teasdale, *Extracting Glueball Masses From Lattice QCD*, *Nucl. Phys.* **B215** (1983) 433.
- [2] G. Parisi, *The Strategy for Computing the Hadronic Mass Spectrum*, *Phys. Rept.* **103** (1984) 203–211.
- [3] G. P. Lepage, *The Analysis of Algorithms for Lattice Field Theory*, in *Theoretical Advanced Study Institute in Elementary Particle Physics*, 6, 1989.
- [4] R. Gupta, S. Park, M. Hoferichter, E. Mereghetti, B. Yoon, and T. Bhattacharya, *Pion–Nucleon Sigma Term from Lattice QCD*, *Phys. Rev. Lett.* **127** (2021), no. 24 242002, [[arXiv:2105.12095](#)].
- [5] L. Barca, G. Bali, and S. Collins, *Toward N to $N\pi$ matrix elements from lattice QCD*, *Phys. Rev. D* **107** (2023), no. 5 L051505, [[arXiv:2211.12278](#)].
- [6] G. Backus and F. Gilbert, *The resolving power of gross earth data*, *Geophysical Journal International* **16** (1968), no. 2 169–205.
- [7] M. Hansen, A. Lupo, and N. Tantalo, *Extraction of spectral densities from lattice correlators*, *Phys. Rev.* **D99** (2019), no. 9 094508, [[arXiv:1903.06476](#)].
- [8] G. Bailas, S. Hashimoto, and T. Ishikawa, *Reconstruction of smeared spectral function from Euclidean correlation functions*, *PTEP* **2020** (2020), no. 4 043B07, [[arXiv:2001.11779](#)].
- [9] A. Barone, S. Hashimoto, A. Jüttner, T. Kaneko, and R. Kellermann, *Inclusive semi-leptonic $B_{(s)}$ mesons decay at the physical b quark mass*, in *39th International Symposium on Lattice Field Theory*, 11, 2022. [arXiv:2211.15623](#).
- [10] A. Rothkopf, *Inverse problems, real-time dynamics and lattice simulations*, *EPJ Web Conf.* **274** (2022) 01004, [[arXiv:2211.10680](#)].
- [11] J. Bulava, M. T. Hansen, M. W. Hansen, A. Patella, and N. Tantalo, *Inclusive rates from smeared spectral densities in the two-dimensional $O(3)$ non-linear σ -model*, *JHEP* **07** (2022) 034, [[arXiv:2111.12774](#)].
- [12] P. Gambino, S. Hashimoto, S. Mächler, M. Panero, F. Sanfilippo, S. Simula, A. Smecca, and N. Tantalo, *Lattice QCD study of inclusive semileptonic decays of heavy mesons*, *JHEP* **07** (2022) 083, [[arXiv:2203.11762](#)].
- [13] R. Frezzotti, N. Tantalo, G. Gagliardi, F. Sanfilippo, S. Simula, and V. Lubicz, *Spectral-function determination of complex electroweak amplitudes with lattice QCD*, *Phys. Rev. D* **108** (2023), no. 7 074510, [[arXiv:2306.07228](#)].
- [14] J. Bulava, *The spectral reconstruction of inclusive rates*, *PoS LATTICE2022* (2023) 231, [[arXiv:2301.04072](#)].

- [15] J. Bulava, A. D. Hanlon, B. Hörz, C. Morningstar, A. Nicholson, F. Romero-López, S. Skinner, P. Vranas, and A. Walker-Loud, *Elastic nucleon-pion scattering at $m_\pi = 200$ MeV from lattice QCD*, *Nucl. Phys. B* **987** (2023) 116105, [[arXiv:2208.03867](#)].